Mitigation of Voltage Mismatches using PSO Based Buck & Boost Converter for Grid Connected PV Inverter

Dr.V.Praveen[1], A.Sai Divya[2], S.Naveena[3], V.Raju Naik[4], P.Chandrika[5]
[1]Associate Professor, Dept of EEE, [2345]Students, A.P Dept of EEE,
[12345]PSCMR College of Engineering & Technology, Vijayawada

Abstract- In this paper, a molecule swarmimprovement (PSO)- based MPPT calculation for PV arrays in confounded ecological conditions is proposed. A solitary phase grid associated transformer less photograph voltaic (PV) inverter which can work either in buck or in boost mode, and can separate maximum power at the same time from two sequentially associated subarrays while each of the sub array is confronting diverse natural conditions, is displayed in this paper. As the inverter can work in buck just as in boost mode relying upon the prerequisite, the limitation on the base number of sequentially associated solar PV modules that is required to frame a sub array is enormously diminished. Accordingly power yield from each of the sub array increments when they are presented to various natural conditions. The topological configuration of the inverter and its control procedure are structured so the high frequency components are absent in the regular mode voltage consequently confining the greatness of the leakage current related with the PV arrays inside as far as possible. Further, high working productivity is accomplished all through its working reach. A point by point examination of the system prompting the advancement of its mathematical model is completed. The suitability of the plan is affirmed by performing point by point simulation examines.

Index Terms- Grid connection, Single phase, Transformerless, Buck & Boost based PV inverter, Maximum power point, PSO, Mismatched environmental condition, Series connected module.

I.   INTRODUCTION

The major concern of a photo voltaic (PV) system is to ensure optimum performance of individual PV modules in a PV array while the modules are exposed to different environmental conditions arising due to difference in insolation level and/or difference in operating temperature. The presence of mismatch in operating condition of modules significantly reduces the power output from the PV array [1]. The problem with the mismatched environmental conditions (MEC) becomes significant if the number of modules connected in series in a PV array is large. In order to achieve desired magnitude for the input dc link voltage of the inverter of a grid connected transformerless PV system, the requirement of series connected modules becomes high. Therefore, the power output from a grid connected transformerless (GCT) PV system such as single phase GCT (SPGCT) inverter based systems derived from H-bridge [2], [3] and neutral point clamp (NPC) inverter based systems [4], [5] get affected significantly during MEC.

In order to address the problem arising out of MEC in a PV system, various solutions are reported in the literature. An exhaustive investigation of such techniques has been presented in [6]. Power extraction during MEC can be increased by choosing proper interconnection between PV modules [6], [7] or by tracking global maximum power point (MPP) of PV array by employing complex MPP tracking (MPPT) algorithm [6], [8]. However, these techniques are not effective for low power SPGCT PV system. Similarly, reconfiguration of the PV modules in a PV array by changing the electrical connection of PV modules [9], [10] is not effective for SPGCT PV system due to the considerable increment in component count and escalation in operating complexity. In order to extract maximum power from each PV module during MEC, attempts have been made to control each PV module in a PV array either by having a power electronic equalizer [11] or by interfacing a dc to dc converter [1], [12]- [14]. Schemes utilizing power electronic equalizer require large component count thereby increasing the cost and operation complexity of the system. The scheme presented in [1] uses generation control circuit (GCC) to operate each PV module at their respective MPP wherein the difference in power between each module is only processed through the GCC.

Scheme presented in [12] uses shunt current compensation of each module as well as series voltage compensation of each PV string in a PV array to enhance power yield during MEC. The schemes based on module integrated converter [13], [14] use dedicated dc to dc converter integrated with each PV module. However, the efficiency of the aforesaid schemes are low due to the involvement of large number of converter stages, and further in these schemes the component count is high and hence they face similar limitations as that of power electronic equalizer based scheme. Instead of ensuring MPP operation of each and every module, certain number of modules are connected in series to form a string and the so formed strings are then made to operate under MPP in [15], [16]. Even then there is not much reduction in overall component count and control complexity [6].

In order to simplify the control configuration and to reduce the component count, schemes reported in [17], [18] combine all the PV modules into two subarrays, and then each of the subarrays is made to operate at their respective MPP. However, the reported overall efficiency of both the schemes is poor. By introducing a buck and boost stage in SPGCT PV inverter, power extraction during MEC is improved in. Further, as a consequence of the presence of the intermediate boost stage, the requirement of series connected PV modules in a PV array has become less. In the schemes presented in [19]- [21], the switches of either the dc to dc converter stage or inverter stage operate at high frequency, as a result there is a considerable reduction in the size of the passive element count, thereby improving the operating efficiency of these schemes. Further, the reported efficiency of and is 1-2 % higher than that of.

An effort has been made in this paper to divide the PV modules into two serially connected subarrays and controlling each of the subarrays by means of a buck and boost based inverter so that optimum power evacuation from the subarrays is ascertained during MEC. This process of segregation of input PV array into two subarrays reduces the number of series connected modules in a subarray almost by half compared to that of the schemes proposed in.

The topological structure and control strategy of the proposed inverter ensure that the magnitude of leakage current associated with the PV arrays remains within the permissible limit. Further, the voltage stress across the active devices is reduced almost by half compared to that of the schemes presented in, hence very high frequency operation without increasing the switching loss is ensured. High frequency operation also leads to the reduction in the size of the passive elements. As a result the operating efficiency of the proposed scheme is high. The measured peak efficiency and the European efficiency (η_{euro}) of the proposed scheme are found to be 97.65% and 97.02% respectively.

II.   PROPOSED INVERTER AND ITS OPERATION

The schematic of the proposed Dual Buck & Boost based Inverter (DBBI) which is depicted in Fig. 1 is comprising of a dc to dc converter stage followed by an inverting stage. The dc to dc converter stage has two dc to dc converter segments, CONV1 and CONV2 to service the two subarrays, P V1 and PV2 of the solar PV array. The segment, CONV1 is consisting of the self-commutated switches, S1 along with its anti-parallel body diode, D1, S3 along with its anti-parallel body diode, D3, the freewheeling diodes, Df1, Df3 and the filter inductors and capacitors, L1, Cf1, and Co1.

Similarly, the segment, CONV2 is consisting of the self-commutated switches, S2 along with its anti-parallel body diode, D2, S4 along with its anti-parallel body diode, D4, the freewheeling diodes, Df2, Df4 and the filter inductors and capacitors, L2, Cf2, and Co2. The inverting stage is consisting of the self-commutated switches, S5, S6, S7, S8, and their corresponding body diodes, D5, D6,D7 and D8 respectively. The inverter stage is interfaced with the grid through the filter inductor, Lg. The PV array to the ground parasitic capacitance is modeled by the two capacitors, Cpv1 and C pv2.
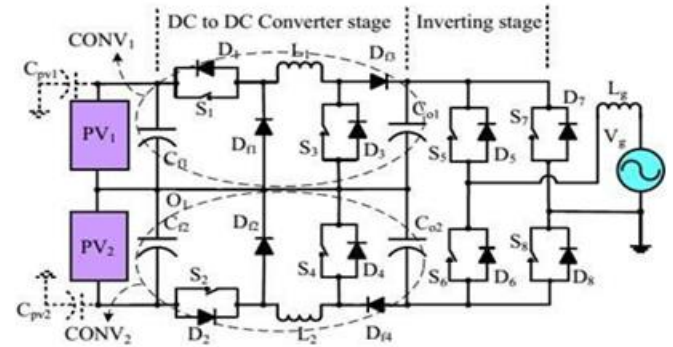

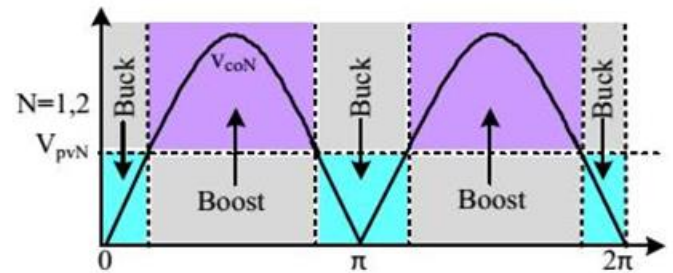
Fig.1: Dual Buck & Boost based Inverter (DBBI)


Fig.2: Buck stage and Boost stage of the proposed inverter

Considering Fig. 2, CONV1 operates in buck mode when V pv1 ≥ vco1, while CONV2 operates in buck mode when V pv2 ≥ vco2. Vpv1, Vpv2 are the MPP voltages of P V1 and P V2 and v co1, vco2 are the output voltages of CONV1 and CONV2 respectively. During buck mode duty ratios of the switches, S1 and S2 are varied sinusoidally to ensure sinusoidal grid current (ig) while S3 and S4 are kept off. When Vpv1 < vco1, CONV1 operates in boost mode while CONV2 operates in boost mode when V pv2 < vco2. During boost mode duty ratios of the switches, S3 and S4 are varied sinusoidally to ensure sinusoidal i g while S1 and S2 are kept on throughout this mode. The sinusoidal switching pulses of the switches of CONV1 and CONV2 are synchronized with the grid voltage, v g to accomplish unity power factor operation. The switches, S5 and S8 are kept on and switches S6 and S7 are kept off permanently during the entire positive half cycle (PHC) while during entire negative half cycle (NHC), the switches, S6 and S7 are kept on and switches, S5 and S8 are kept off permanently. All the operating states of the proposed inverter are depicted in Fig. 3.
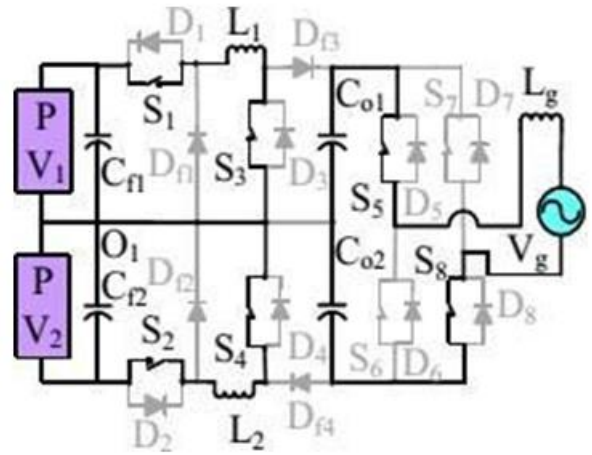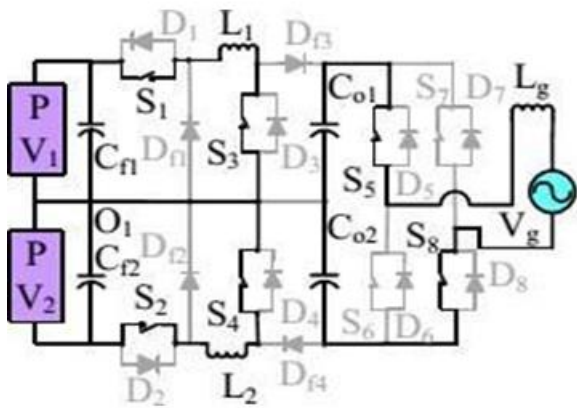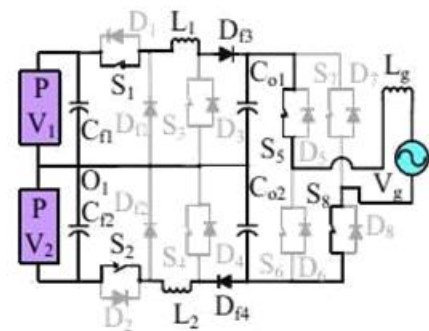
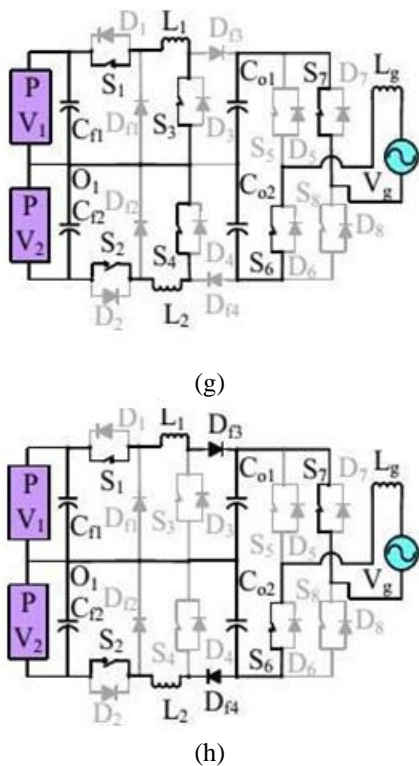(a)

(b)

(c)

(d)

(e)

(f)

(g)

(h)
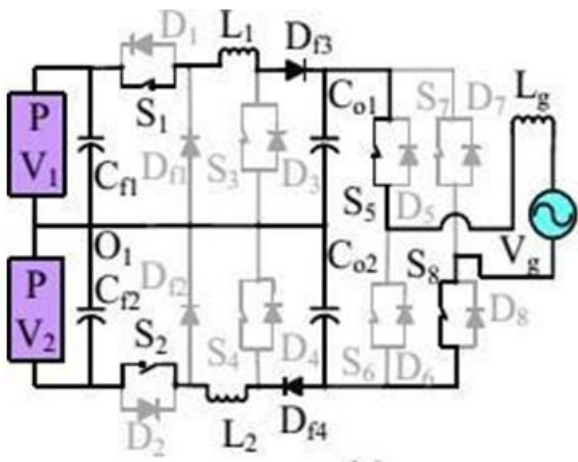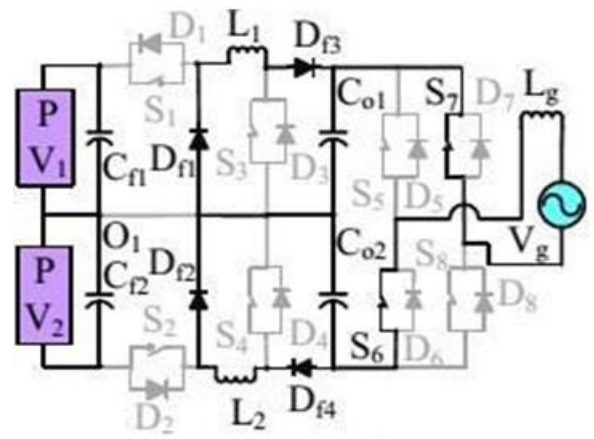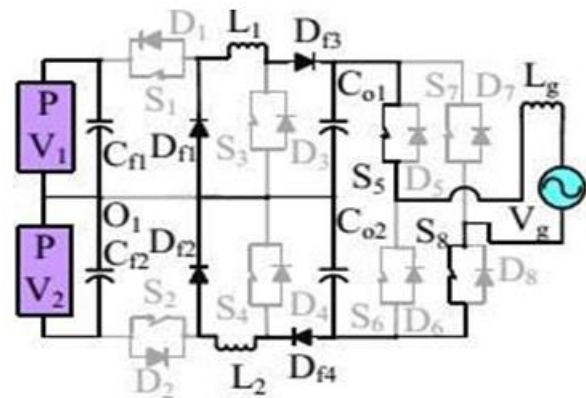
Fig. 3 Operating states of DBBI: (a) Active and (b) Freewheeling states in buck mode of PHC, (c) Active and (d) Freewheeling states in buck mode of NHC, (e) Active and (f) Freewheeling states in boost mode of PHC, (g) Active and (h) Freewheeling states in boost mode of NHC When the insolation level and ambient temperature of sub array P V1 are different from that of P V2, the MPP parameter of the two subarrays, Vpv1 and Vpv2, MPP current, Ipv1 and Ipv2 correspond to PV1 and PV2 respectively and power at MPP, Ppv1 and Ppv2 correspond to PV1 and PV2 respectively differ from each other. By considering that both the subarrays are operating at their respective MPP and neglecting the losses incurred in power processing stages, the average power involved with C o1 and Co2, Pco1 and Pco2 over a half cycle can be assumed equal to the power extracted from PV1 and PV2. Therefore,

$$=1 \quad \&2 \ =2 \tag{1}$$

The power injected to the grid averaged over a half cycle, Pg can be written as

$$= \quad 1+ \quad 2 \tag{2}$$

Further, at any half cycle

$$= \quad 1+ \quad 2 \tag{3}$$

Hence, the instantaneous injected power to the grid, pg can be written as

$$==(\quad 1+ \quad 2) \tag{4}$$

Where in vco1 and vco2 denote the instantaneous

quantities of Vco1 and Vco2 respectively. As ig is in-phase with vg, Where in Vg and Ig denote rms values of vg and ig respectively. The power injected to the grid can be expressed as Where in the amplitudes of vco1, vco2 and ig are denoted as Vco1m, Vco2m and Igm respectively. Combining (1), (8) and (9) where in the amplitudes of vco1, vco2 and ig are denoted as V co1m, Vco2m and Igm respectively. Combining (1), (8) and (9) The voltage templates of vco1 and vco2 appear as full wave rectified sinusoidal waveform with amplitudes, Vco1m and Vco2m respectively. Vm is the amplitude of vg. It can be deduced from (12) that the magnitudes of Vco1m and Vco2m are decided by the power extracted from each of the subarray. If the power extracted from PV1 is less than PV2, then V co1m < Vco2m, whereas Vco2m < Vco1m if power extracted from PV2 is less than PV1. During buck mode, the duty ratios, d1 of S1 and d2 of S2 vary sinusoidally with an amplitude d1m and d2m, where in While during boost mode the duty ratios, d3 of S3 and d4 of S4 vary sinusoidally with amplitude d3m and
d4m, wherein

$$= 1 - \quad 1 \qquad \& \qquad \overline{\quad = 1 -} \quad 2 \tag{7}$$

$$3 \qquad 14 \qquad 2$$

The CONV1 and CONV2 are having the same output current ig. Hence, the input side currents before getting filtered by input filter capacitors of CONV1, isw1 and CONV2, isw2 can be related with ig in the buck mode by considering the switching cycle average of corresponding quantities as follows Similarly by considering switching cycle average of corresponding quantities the relation between isw1, isw2 and ig can be deduced during boost mode as Therefore, it can be inferred from (12) and (13) that if the insolation level of PV1 is lower than that of PV2, during buck mode, d1m < d2m, thereby hd1iT s < hd2iT s whereas during boost mode as per (12) and (14), d3m < d4m, thereby hd3iT s < hd4iT s . Hence, it can be concluded from (15), (16), (17) and (18) that in any operating mode, hisw1iT s < hisw2iT s , therefore I pv1< Ipv2. Following the same argument, Ipv1 > I pv2 if the insolation level of PV1 is higher than that of PV2. Considering Fig. 1 it can be noted that during operation in PHC, vcpv1 = vco2 + Vpv1, vcpv2 = vco2
− Vpv2 while during NHC vcpv1 = −vco1 + Vpv1, vcpv2 = −vco1 − Vpv2, wherein vcpv1 and vcpv2 are the voltages impressed across Cpv1 and Cpv2 respectively.

III. MATHEMATICAL MODEL OF THE PROPOSED SCHEME

A small signal modeling of the proposed inverter has been carried out for buck mode and boost mode of operation. Fig. 4(a) and (b) represent the equivalent circuit of the proposed inverter while it operates in buck mode whereas Fig. 4(c) and

(d) represent the equivalent circuit of the converter while it operates in boost mode. RL1, RL2, Rg, Rco1 and Rco2 are the parasitic resistances of L1, L2, Lg, Co1 and Co2 respectively. As indirect grid current control method is adopted to control ig, the quantities iL1, iL2, vco1, vco2 and ig are considered to be the state variables. The state equations representing the buck mode of operation of the inverter are derived to be (19), (20) by considering the equivalent circuits of Fig. 4(a), (b) while the state equations for boost mode are derived to be (21), (19) by considering the equivalent circuits of Fig. 4(c), (d).

$$
\begin{bmatrix} \dot{i}_{L1}(t) \\ \dot{i}_{L2}(t) \\ \dot{v}_{co1}(t) \\ \dot{v}_{co2}(t) \\ \dot{i}_g(t) \end{bmatrix} = \begin{bmatrix} -\frac{R_{L1}+R_{co1}}{L_1} & 0 & -\frac{1}{L_1} & 0 & \frac{R_{co1}}{L_1} \\ 0 & -\frac{R_{L2}+R_{co2}}{L_2} & 0 & -\frac{1}{L_2} & \frac{R_{co2}}{L_2} \\ \frac{1}{C_{o1}} & 0 & 0 & 0 & -\frac{1}{C_{o1}} \\ 0 & \frac{1}{C_{o2}} & 0 & 0 & -\frac{1}{C_{o2}} \\ \frac{R_{co1}}{L_g} & \frac{R_{co2}}{L_g} & \frac{1}{L_g} & \frac{1}{L_g} & -\frac{R_{co1}+R_{co2}+R_g}{L_g} \end{bmatrix} \begin{bmatrix} i_{L1}(t) \\ i_{L2}(t) \\ v_{co1}(t) \\ v_{co2}(t) \\ i_g(t) \end{bmatrix} + \begin{bmatrix} \frac{1}{L_1} & 0 & 0 \\ 0 & \frac{1}{L_2} & 0 \\ 0 & 0 & 0 \\ 0 & 0 & 0 \\ 0 & 0 & -\frac{1}{L_g} \end{bmatrix} \begin{bmatrix} v_{pv1}(t) \\ v_{pv2}(t) \\ v_g(t) \end{bmatrix}
$$

(19)

$$
\begin{bmatrix} \dot{i}_{L1}(t) \\ \dot{i}_{L2}(t) \\ \dot{v}_{co1}(t) \\ \dot{v}_{co2}(t) \\ \dot{i}_g(t) \end{bmatrix} = \begin{bmatrix} -\frac{R_{L1}+R_{co1}}{L_1} & 0 & -\frac{1}{L_1} & 0 & \frac{R_{co1}}{L_1} \\ 0 & -\frac{R_{L2}+R_{co2}}{L_2} & 0 & -\frac{1}{L_2} & \frac{R_{co2}}{L_2} \\ \frac{1}{C_{o1}} & 0 & 0 & 0 & -\frac{1}{C_{o1}} \\ 0 & \frac{1}{C_{o2}} & 0 & 0 & -\frac{1}{C_{o2}} \\ \frac{R_{co1}}{L_g} & \frac{R_{co2}}{L_g} & \frac{1}{L_g} & \frac{1}{L_g} & -\frac{R_{co1}+R_{co2}+R_g}{L_g} \end{bmatrix} \begin{bmatrix} i_{L1}(t) \\ i_{L2}(t) \\ v_{co1}(t) \\ v_{co2}(t) \\ i_g(t) \end{bmatrix} + \begin{bmatrix} 0 & 0 & 0 \\ 0 & 0 & 0 \\ 0 & 0 & 0 \\ 0 & 0 & 0 \\ 0 & 0 & -\frac{1}{L_g} \end{bmatrix} \begin{bmatrix} v_{pv1}(t) \\ v_{pv2}(t) \\ v_g(t) \end{bmatrix}
$$

(20)

$$
\begin{bmatrix} \dot{i}_{L1}(t) \\ \dot{i}_{L2}(t) \\ \dot{v}_{co1}(t) \\ \dot{v}_{co2}(t) \\ \dot{i}_g(t) \end{bmatrix} = \begin{bmatrix} -\frac{R_{L1}}{L_1} & 0 & 0 & 0 & 0 \\ 0 & -\frac{R_{L2}}{L_2} & 0 & 0 & 0 \\ 0 & 0 & 0 & 0 & -\frac{1}{C_{o1}} \\ 0 & 0 & 0 & 0 & -\frac{1}{C_{o2}} \\ 0 & 0 & \frac{1}{L_g} & \frac{1}{L_g} & -\frac{R_{co1}+R_{co2}+R_g}{L_g} \end{bmatrix} \begin{bmatrix} i_{L1}(t) \\ i_{L2}(t) \\ v_{co1}(t) \\ v_{co2}(t) \\ i_g(t) \end{bmatrix} + \begin{bmatrix} \frac{1}{L_1} & 0 & 0 \\ 0 & \frac{1}{L_2} & 0 \\ 0 & 0 & 0 \\ 0 & 0 & 0 \\ 0 & 0 & -\frac{1}{L_g} \end{bmatrix} \begin{bmatrix} v_{pv1}(t) \\ v_{pv2}(t) \\ v_g(t) \end{bmatrix}
$$

(21)

The state space averaging based technique is adopted as the grid frequency; fg is adequately lower than the switchin frequency, fs. In order to simplify the analysis, Vpv1, Vpv2 and vg are considered as stiff voltage sources, and the effect of input filter capacitors is neglected. The values of the system parameters are considered to be as follows: RL1 = RL2 = 0.12 Ω, Rg = 0.04 Ω, Rco1 = Rco2 = 0.26 Ω, Vpv1 = Vpv2 = 130 V. Considering symmetry in operation of CONV1 and CONV2, and by applying state space averaging technique to (19), (20) and (21), the simplified transfer functions of ig(s)/d(s), iL1(s)/d(s) and vco1(s)/d(s) in s-domain during buck mode are obtained as
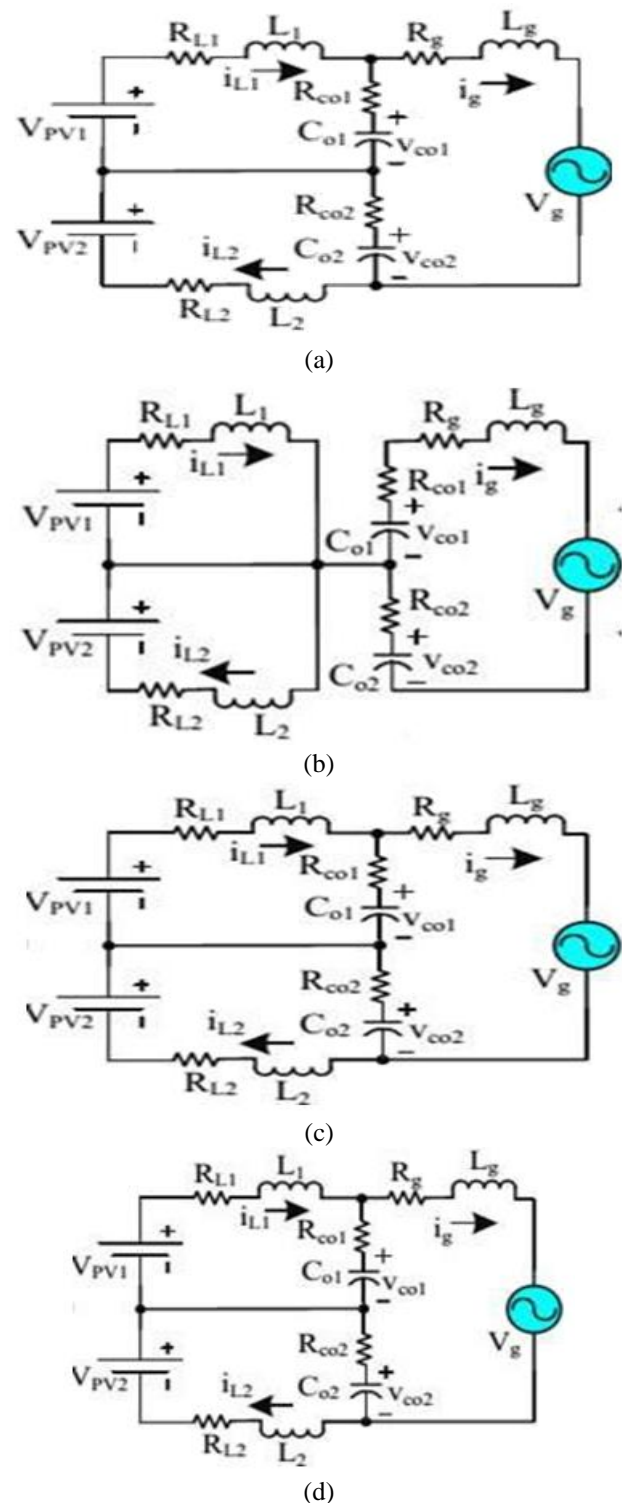

(a)

(b)

(c)

(d)

Fig. 4 Equivalent circuit in Buck mode (a) S1, S2 are ON (b) S1, S2 are OFF, in Boost mode (c) S3, S4 are ON (d) S3, S4 are OFF

IV. CONTROL STRATEGY OF THE PROPOSED SCHEME

The control strategy of the proposed scheme is depicted in Fig. 5. The controller is designed to fulfil the following objectives: i) both subarrays operate at their corresponding MPP simultaneously, ii) sensing of output voltages, vco1 and v co2 are not required, iii) ig is sinusoidal and is in-phase with v g throughout the operating range. Two separate MPP trackers and two proportional integral (PI) controllers are employed to determine the value of P pv1 and Ppv2 which are required
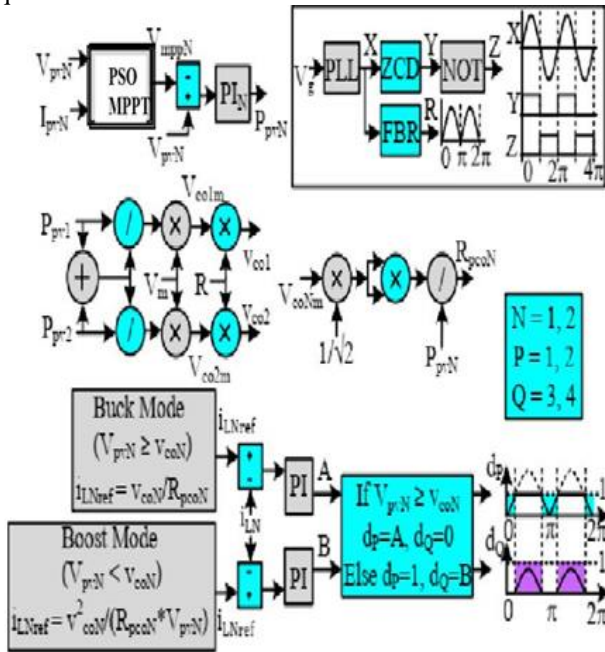

Fig.5: Control configuration of the proposed inverter to estimate Vco1m and Vco2m

Using (12), Vco1m and Vco2m are determined where the information of V m is obtained from the phase locked loop (PLL). A rectified version of a unity sinusoidal function, R is generated from a unity sinusoidal function, X, synchronized with vg, and is obtained from the same PLL. R is multiplied with Vco1m and Vco2m to estimate v co1 and vco2. Hence, two voltage sensors which otherwise would have been required to determine vco1 and vco2 get eliminated. V pv1 and vco1 are compared to decide about the mode ofoperation (buck mode or boost mode) of CONV1, while Vpv2 and vco2 are compared to determine the mode of operation of CONV2. RMS values of vco1 and vco2 are estimated which are then subsequently squared and are then divided by Ppv1 and Ppv2 to obtain the emulated effective resistances, Rpco1 and Rpco2 of the two component converters. Subsequently the reference current, iL1ref of L1 and the reference current, iL2ref of L2,

are synthesized by utilizing While for boost mode (23) is used to generate iL1ref and iL2ref.

The sensed inductor currents, iL1 and iL2 are compared with their corresponding references iL1ref and iL2ref. The errors so obtained are processed through two separate PI controllers to generate the required sinusoidal duty ratios for the switches, S1 and S2 during buck mode. Similarly, two separate PI controllers are engaged to process the generated errors to synthesize required sinusoidal duty ratios for switches S3 and S4 during boost mode.

V. SELECTION OF L1, L2, Lg& Co1, Co2

In order to select the value of the filter elements, L1, L2, Lg& Co1, Co2 the design principle given in is followed and the buck mode of operation for the inverter is considered. Values of L1 and L2 are obtained from the expression given in wherein, Vpv1 = Vpv2 = 200 V, percentage peak to peak ripple of iL1 and iL2, $\Delta IL1$ and $\Delta IL2$ are considered as 15% of rated peak current.

VI. OVERVIEW OF THE PSO ALGORITHM

PSO is a swarm intelligence optimization algorithm developed by Eberhart and Kennedy in 1995. In this algorithm, several cooperative agents are used, and each agent exchanges information obtained in its respective search process. Each agent, referred to as a particle, follows two very simple rules, i.e., to follow the best performing particle, and to move towards the best conditions found by the particle itself. By this way, each particle ultimately evolves to an optimal or close to optimal solution. The standard PSO m

$$(+ 1) = \quad ( ) +_{1 1}.(\quad . - ( )) +$$
$$_{2 2}.(\quad . - ( )) \qquad (26)$$
$$(+ 1) = \quad ( ) + \quad (+ 1) \qquad (27)$$
$$I=1,2,\ldots\ldots,N$$

Where xi is the position of particle i; vi is the velocity of particle i; k denotes the iteration number; w is the inertia weight; r1 and r2 are random variables uniformly distributed within [0,1]; and c1, c2 are the cognitive and social coefficient, respectively. The variable pbest,i is used to store the best position that the i-th particle has found so far, and gbest is used to store the best position of all the particles.

Step1.

PSO initialization Particles are usually initialized randomly following a uniform distribution over the search space, or are initialized on grid nodes that cover the search space with equidistant points. Initial velocities are taken randomly.

Step2. Fitness Evaluation Evaluate the fitness value ofeach particle. Fitness evaluation is conducted by supplying the candidate solution to the objective function.

Step3. Update individual and global best dataIndividual and global best fitness values (pbest,i and gbest) and positions are updated by comparing the newly calculated fitness values

against the previous ones, and replacing the pbest,i and gbest as well as their corresponding positions as necessary.

Step4. Update velocity and position of each particlethe velocity and position of each particle in the swarm is updated using Eq. (2) and (3).

Step5. Convergence Determination Check theconvergence criterion. If the convergence criterion is met, the process can be terminated; otherwise, the iteration number will increase by 1 and goto step 2.

VII. SIMULATION STUDY

To demonstrate the efficacy of the proposed inverter a PV array consisting of two PV subarrays while each of the subarray having four series connected Canadian solar polycrystalline modules „CS6P-165PE" is considered. The MPP parameters of each subarray at standard test condition (STC) are as follows: Vpv1 = Vpv2 = 116 V, Ipv1 = Ipv2 = 5.7 A and P pv1 = Ppv2 = 661 W. The parameters which are used to simulate *the* proposed inverter are indicated in Table I.

TABLE I
Employed Parameters/Elements For Simulation And Experimental Purpose

& 1, 2, & 1, 2	220V and 50Hz 0.6mH,0.6Mh, 0.4Mh
1·2	0.1µF
MPPT Algorithm	PSO
IGBT (1−8)	IPW60R041C6
Diodes(1−4)	MBR40250
81 − 4 &	
85 − 8	50 kHz & 50 Hz
Digital Signal Controller	TMS320F28335

Matlab Simulink platform is utilized to simulate the performance of the proposed inverter.The variation in insolation level and temperature with respect to time range of operation which is considered for the two subarrays to demonstrate the effectiveness of the proposed inverter are tabulated in Table II.
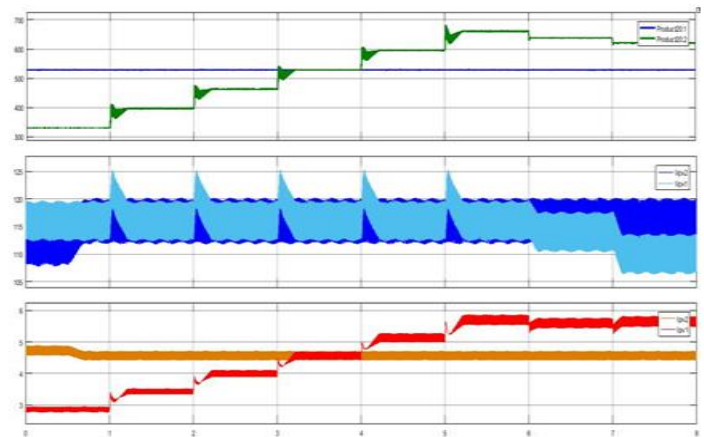

Fig. 6. Simulated waveform: Variation in (a) ppv1 and ppv2, (b) vpv1 and v pv2, (c) ipv1 and ipv2 during entire range of operation

TABLE II
Estimated Variations of Different Quantities during Applied Variations on Insolation and Temperature of Two Subarrays

Time in Second	0-1	1-2	2-3	3-4	4-5	5-6	6-7	7-8
Insol. in PV_1 (kW/m^2)	0.5	0.6	0.7	0.8	0.9	1.0	1.0	1.0
Insol. in PV_2 (kW/m^2)	0.8	0.8	0.8	0.8	0.8	0.8	0.8	0.8
Temp. in PV_1 (°C)	25	25	25	25	25	25	30	35
Temp. in PV_2 (°C)	25	25	25	25	25	25	25	25
P_{pv1} (W)	331	397	463	529	595	661	638	621
P_{pv2} (W)	529	529	529	529	529	529	529	529
I_{gm} (A)	5.5	6.0	6.4	6.8	7.2	7.7	7.5	7.4
V_{co1m} (V)	120	133	147	155	165	173	170	168
V_{co2m} (V)	191	178	164	156	146	138	141	143
I_{L1m} (A)	5.7	7	8.1	9	10.3	11.4	11	10.7
I_{L2m} (A)	9	9	9	9	9	9	9	9

Estimated variation of Ppv1, Ppv2 along with the other parameters Igm, Vco1m, Vco2m, peak of iL1 (IL1m) and peak of iL2 (IL2m) are also indicated in the same table. Fig. 6(a)-(c) represents the variation of Ppv1, Ppv2, Vpv1, V pv2, Ipv1, Ipv2 of the two subarrays and also demonstratesthe ability of the proposed inverter to operate the two subarrays simultaneously at their respective MPP. Variation in ig, iL1, iL2, vco1 and vco2 along with their magnified versions for two different insolation levels are depicted in Figs. 7 to 9. The estimated values of the aforementioned quantities as tabulated in Table II conform to that of obtained through simulation studies thereby ensuring the viability of the proposed scheme.
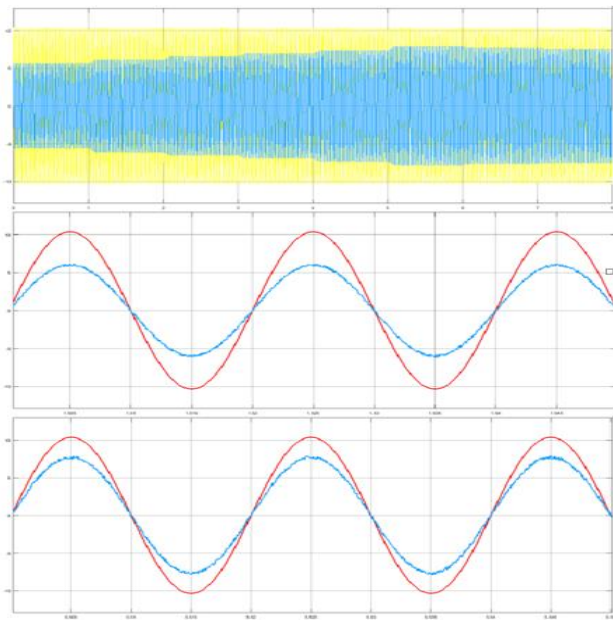
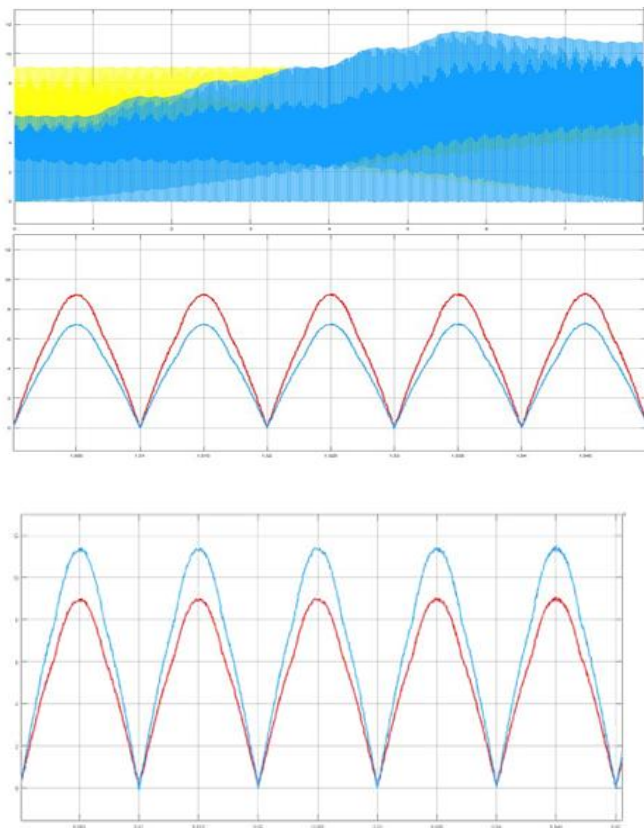Fig.7.Simulated waveform: vg and ig and their magnified views

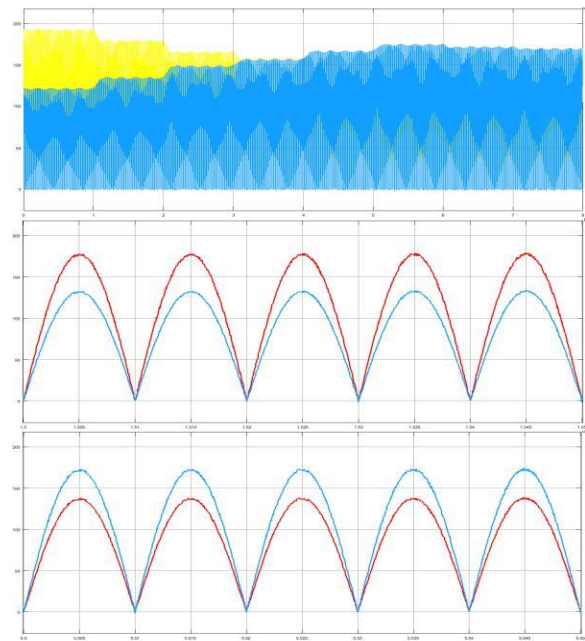Fig. 8.Simulated waveform: iL1 and iL2 and their magnified views

Fig. 9 Simulated waveform: vco1 and vco2 and their magnified views

VIII. CONCLUSION

A solitary phase grid associated transformerless buck and boost based PV inverter which can work two subarrays at their particular PSO MPPT based proposed in this paper. PSO procedures can produce fantastic arrangements inside shorter figuring time and stable union qualities than other stochastic methods.The attractive highlights of this inverter were

I) impact of confounded natural conditions on the PV array could be managed in a compelling way, ii) working proficiency accomplished, $\eta euro = 97.02\%$ was high, iii) decoupled control of component converters was conceivable, iv) basic MPPT calculation was utilized to guarantee MPP operation for the component converters, v) leakage current related with the PV arrays was inside the farthest point referenced in VDE 0126-1-1. Mathematical examination of the proposed inverter prompting the advancement of its little signal model was completed. The model to choose the estimations of the output filter components was displayed. The plan was approved via completing definite simulation contemplates.

IX. REFERENCES

[1]. T. Shimizu, O. Hashimoto, and G. Kimura, "A novel high-performance utility-interactive photovoltaic inverter system," IEEE Trans. Power Electron., vol. 18, no. 2, pp. 704-711, Mar. 2003.

[2]. S. V. Araujo, P. Zacharias, and R. Mallwitz, "Highly efficient single phase transformerless inverters for grid-connected photovoltaic systems," IEEE Trans. Ind. Electron., vol. 57, no. 9, pp. 3118-3128, Sep. 2010.

[3]. B. Ji, J. Wang, and J. Zhao, "High-efficiency single-phase transformerless PV H6 inverter with hybrid modulation method," IEEE Trans. Ind. Electron., vol. 60, no. 5, pp. 2104-2115, May 2013. [4] R. Gonzalez, E. Gubia, J. Lopez, and L. Marroyo,

[4]. "Transformerless single phase multilevel-based photovoltaic inverter," IEEE Trans. Ind. Electron., vol. 55, no. 7, pp. 2694-2702, Jul. 2008.

[5]. H. Xiao and S. Xie, "Transformerless split-inductor neutral point clamped three-level PV grid-connected inverter," IEEE Trans. Power Electron., vol. 27, no. 4, pp. 1799-1808, Apr. 2012.

[6]. A. Bidram, A. Davoudi, and R. S. Balog, "Control and circuit techniques to mitigate partial shading effects in photo voltaic arrays," IEEE J. Photovolt., vol. 2, no. 4, pp. 532-546, Oct. 2012.

[7]. N. D. Kaushika, and N. K. Gautam, "Energy yield simulations of interconnected solar PV arrays," IEEE

[8]. Trans. Energy Convers., vol. 18, no. 1, pp. 127-134, Mar. 2003. H. Patel, and V. Agarwal, "Maximum power point tracking scheme for PV systems operating under partially shaded conditions," IEEE Trans. Ind. Electron., vol. 55, no. 4, pp. 1689-1698, Apr. 2008.

[9]. D. Nguyen, and B. Lehman, "An adaptive solar photovoltaic array using model-based reconfiguration algorithm," IEEE Trans. Ind. Electron., vol. 55, no. 7, pp. 2644-2654, Jul. 2008.

[10]. G. V.-Quesada, F. G.-Gispert, R. P.-Lopez, M. R.-Lumbreras, and A. C.- Roca, "Electrical PV array reconfiguration strategy for energy extraction improvement in grid-connected PV systems," IEEE Trans. Ind. Electron., vol. 56, no. 11, pp. 4319-4331, Nov. 2009.

[11]. L. F. L. Villa, T.-P. Ho, J.-C. Crebier, and B. Raison, "A power electronics equalizer application for partially shaded photovoltaic modules," IEEE Trans. Ind. Electron., vol. 60, no. 3, pp. 1179-1190, Mar. 2013.

[12]. P. Sharma, and V. Agarwal, "Maximum power extraction from a partially shaded PV array using shunt-series compensation," IEEE J. Photovolt., vol. 4, no. 4, pp. 1128-1137, Jul. 2014.

[13]. N. Femia, G. Lisi, G. Petrone, G. Spagnuolo, and M. Vitelli, "Distributed maximum power point

[14]. tracking of photovoltaic arrays: novel approach and system analysis," IEEE Trans. Ind. Electron., vol. 55, no. 7, pp. 2610-2621, Jul. 2008.

[15]. C. Olalla, C. Deline, D. Clement, Y. Levron, M. Rodriguez, and D. Maksimovic, "Performance of power-limited differential power processing architectures in mismatched PV systems," IEEE Trans. Power Electron., vol. 30, no. 2, pp. 618-630, Feb. 2015.

[16]. E. Karatepe, T. Hiyama, M. Boztepe, and M. C. olak, "Voltage based power compensation system for photo voltaic generation system under partially shaded insolation conditions," Energy Convers. and Manage., vol. 49, pp. 2307-2316, Aug. 2008.